Environmental Science Nano

Influence of Functional Groups on the Degradation of Graphene Oxide Nanomaterials

Journal:	*Environmental Science: Nano*
Manuscript ID	EN-ART-03-2019-000355.R1
Article Type:	Paper
Date Submitted by the Author:	24-May-2019
Complete List of Authors:	Shams, Mehnaz; Washington State University, Civil and Environmental Engineering Guiney, Linda; Northwestern University, Department of Materials Science and Engineering Huang, Lijuan; Nanjing Tech University, College of Chemical Engineering Ramesh, Mani; Northwestern University, Department of Materials Science and Engineering Yang, Xiaoning; Nanjing Tech University, College of Chemical Engineering Hersam, Mark; Northwestern University, Department of Materials Science and Engineering Chowdhury, Indranil; Washington State University, Civil and Environmental Engineering

ENVIRONMENTAL SIGNIFICANCE STATEMENT

Graphene nanomaterial is one of the most commonly used carbon-based nanomaterials in the industries. However, degradation of graphene nanomaterials has become an environmental issue. While graphene oxide has been shown to be susceptible to degradation under sunlight, it is still unknown how the various functional groups in graphene oxide nanomaterials can play roles in degradation. In this study, the influence of functional groups on the degradation of graphene nanomaterials under direct sunlight was investigated. The degradation of the nanomaterials was determined to be directly related to the functional groups present on the basal plane of the graphene nanomaterials. Specifically, the hydroxyl and epoxy functional groups are the most susceptible to photodegradation. Upon sunlight exposure, the amount of oxygen-containing functional groups on all graphene nanomaterials decreases over time, with fully reduced graphene oxide showing the lowest degradation rate due to the presence of fewer reactive functional groups on the surface. Overall, these results suggest that the oxygen-containing functional groups on the basal plane are the major initiators of the photodegradation of graphene nanomaterials. This work provides important insight into the role of functional groups in the stability and degradation of graphene nanomaterials, and thus contributes to the design of sustainable applications of these nanomaterials.

Influence of Functional Groups on the Degradation of Graphene Oxide Nanomaterials

Mehnaz Shams[a], Linda M. Guiney[b], Lijuan Huang[c], Mani Ramesh[b], Xiaoning Yang[c], Mark C. Hersam[b], and Indranil Chowdhury[a*]

[a] Department of Civil & Environmental Engineering, Washington State University, Pullman, WA 99164, USA

[b] Departments of Materials Science and Engineering, Chemistry, and Medicine, Northwestern University, Evanston, Illinois 60208, USA

[c] College of Chemical Engineering, Nanjing Tech University, Nanjing, 21108, China

[*]Corresponding Author: indranil.chowdhury@wsu.edu ; 509-335-3721

ABSTRACT

The influence of functional groups on the degradation of graphene oxide nanomaterials under direct sunlight was investigated by systematically varying the surface chemistry. Using a solvothermal reduction process, graphene nanomaterials with varying oxidation levels, including graphene oxide, partially reduced graphene oxide and fully reduced graphene oxide were prepared. The physical and chemical properties of the nanomaterials were extensively characterized before and after exposure to simulated sunlight. The degradation of the nanomaterials was determined to be directly related to the functional groups present on the basal plane of the graphene nanomaterials. Specifically, the hydroxyl and epoxy functional groups are the most susceptible to photodegradation. Upon sunlight exposure, the amount of oxygen-containing functional groups on all graphene nanomaterials decreases over time, with fully reduced graphene oxide showing the lowest degradation rate due to the presence of fewer reactive functional groups on the surface. Overall, these results suggest that the oxygen-containing functional groups on the basal plane are the major initiators of the photodegradation of graphene nanomaterials.

1. INTRODUCTION

Two-dimensional (2D) nanomaterials are being explored for a myriad of applications in the electronic, biomedical, pharmaceutical, cosmetic, energy, and paint industries.[1-5] In particular, graphene and other carbon-based nanomaterials are used in many environmental applications including coatings, catalysis, and as sorbents for water and wastewater treatment.[2, 6] 2D Graphene sheet, whose honeycomb lattice is comprised of sp^2-hybridized carbon atoms, demonstrates unique physical and chemical characteristics.[7] The hexagonal ring structure of graphene resemble polycyclic aromatic hydrocarbons (PAHs) and can be considered as a large sheet of many fused PAHs.[8] Traditional forms of graphene, currently used in different applications, include pristine graphene, graphene oxide (GO), and reduced graphene oxide (rGO). While pristine graphene is often the most desirable for applications, GO and rGO are more commonly used due to their scalable and cost-effective methods of production. GO is an oxidized form of graphene with additional functional groups such as epoxy, hydroxyl, carbonyl, and carboxyl groups covalently bound on the basal planes (for epoxy and hydroxyl groups) or the edges (for carbonyl and carboxyl groups).[9] These functional groups make GO hydrophilic and therefore readily dispersible in water.[10]

The degradation and transformation of graphene nanomaterials need to be well-understood in order to establish their potential environmental risks. For example, graphene can transform and degrade into numerous combinations of PAHs,[11, 12] which are potentially carcinogenic and pose a number of environmental and health risks.[8, 13] Fenton reactions may cause oxidation of graphene materials, [14] while microbial interactions can cause reduction.[15] Hence, multiple types of interactions can be occurring with suspended graphene materials in the environment.[16] Photodegradation is one among several pathways that can cause transformation of graphene

nanomaterials in the environment. Thus, in order to understand the long-term environmental impact of graphene nanomaterials, it is important to study sunlight-mediated photolysis and degradation.

Recent studies have shown that GO can be highly stable against aggregation in a natural aquatic environment,[17, 18] indicating that GO will persist in water where sunlight-mediated photo-transformation can occur.[17, 18] Additionally, this transformation can have an impact on the fate and transport of these materials. Transformation by sunlight photolysis is one of the primary routes by which carbonaceous materials such as fullerenes transform into CO_2 and other oxygen containing functionalities.[19-27] Some recent studies have shown that graphene is photoreactive.[12, 28-30] For example, one study found that GO readily reacts under simulated sunlight exposure, forming fragmented photoproducts that are similar to reduced GO (rGO) as well as low molecular weight (LMW) species. [31] Furthermore, GO photoreactivity involves the simultaneous formation of oxidative and reductive transient species.

To date, studies have investigated only the photodegradation of GO. The influence of functional groups on the degradation process of graphene nanomaterials is still unknown. These knowledge gaps have motivated this study to determine the influence of functional groups on the direct photolysis of graphene nanomaterials. We hypothesize that the degradation of the graphene flakes starts at the basal planes, caused by the presence of the epoxy and hydroxyl functional groups. Thus, we anticipate that the presence, identity, and quantity of these functional groups will influence the degradation process of the materials.[32, 33] Furthermore, we hypothesize that rGO will be more resistant to degradation due to the presence of fewer functional groups and increased hydrophobicity. [16] The fate and transformation of nanomaterials are key factors to consider when determining their environmental risk.[34] This work provides important insight into

the role of functional groups in the stability and degradation of graphene nanomaterials, and thus contributes to the design of sustainable applications of these materials.

2. MATERIALS AND METHODS

2.1 Materials

Graphene oxide materials were synthesized using a modified Hummers' method.[35] To vary the functional groups on the surface, two samples of reduced GO—partially reduced graphene oxide (rGO-2h) and fully reduced graphene oxide (rGO-5h)—were prepared by a solvothermal reduction process. In particular, GO was suspended in N-methyl-2-pyrrolidone (NMP) and heated to 150 °C with constant stirring in a silicone oil bath. The heat reflux was stopped after 2 hours and 5 hours to achieve varying levels of reduction. After the solvothermal reduction, the rGO was separated from the NMP using vacuum filtration with 0.1 μm alumina filters (Millipore), rinsed heavily with DI water, and re-dispersed in DI water at an approximate concentration of 1 mg/mL.[36] All aqueous solutions for irradiation were prepared using Milli-Q (Deionized water ≥ 18 MΩ) water. Each stock solution was diluted to a concentration of 50 mg/L of nanomaterials (GO, rGO-2h, and rGO-5h) in Milli-Q water.

2.2 Photodegradation Studies

All simulated sunlight experiments were carried out in an Atlas SunTest CPS+ solar simulator, equipped with a 1 kW xenon arc lamp. The sunlight experiments were carried out in borosilicate glass tubes (outside diameter = 1.3 cm; volume = 24 mL; conforms to ASTM Type 1, Class A and USP Type 1 Glass) that were filled to 10 ml with the working solutions. The sample tubes

were sealed with open-top caps lined with gastight polytetrafluoroethylene (PTFE) and kept on top of a mesh to keep them submerged in a thermostatic water bath (25 °C) during irradiation. The incident light intensity at the tube surface (300 nm to 800 nm) was 0.065 W/cm^2. For kinetic studies, a series of tubes were prepared for irradiation. Photodegradation tests were continued for 168 h. At specific time points during irradiation, individual tubes were removed from the reactor for chemical analysis. After removal, the tubes were wrapped with aluminum foil and kept in a refrigerator. Dark control tubes were wrapped with aluminum foil and kept under the same experimental conditions. Details of the control study are described in the supporting information.

2.3 Material Characterization

Atomic force microscopy (AFM) was used to monitor the size and morphology of the graphene oxide flakes. The physical dimensions of the GO, including flake thickness and lateral size were quantified from AFM image analysis, as described previously.[36,31] For AFM imaging, silicon wafers were cleaned and dried and then functionalized with a monolayer of (3-aminopropyl) triethoxysilane (APTES) by soaking the wafers in a 2.5 mM solution of APTES in isopropyl alcohol (IPA) for 30 minutes. Following the APTES treatment, the wafers were rinsed with IPA and dried with a nitrogen gun. The GO solutions were bath sonicated for 5 minutes before being drop-casted onto the APTES functionalized wafers. The GO was allowed to sit for 10 minutes on the wafer before being rinsed with water and dried with a nitrogen gun. The samples were then annealed at 250 °C for 30 minutes on a hotplate before imaging with a Cypher Asylum ES AFM.

Ultraviolet (UV)-visible spectroscopy spectra were collected using a Perkin Elmer Lambda 365 UV-visible absorbance spectrophotometer equipped with a 1 cm light path quartz cuvette. Changes in the UV-vis spectra were used to monitor the graphene oxide concentration and changes in light absorption properties.

Zeta potential, hydrodynamic diameter, and polydispersity index of the particles were measured using a Zetasizer Nano ZS (Malvern Instruments, Inc.). A 1 cm light path quartz cuvette was used for size measurements and a folded capillary cell DTS1070 was used for zeta potential measurements. Particle size is determined via the diffusion coefficient, which is then used to calculate particle size, typically as sphere equivalent.[37] Also, calculation of zeta potential values from EPM measurements uses the Smoluchowski equation which assumes spherical particles. Hence, it is recommended to use this approach for spherical particles.[38] Solutions were bath sonicated for 5 minutes preceding measurement.

XPS was utilized to determine the chemical composition of the graphene nanomaterials. For XPS, approximately 5 mg of GO or rGO in DI water were deposited 1 μm PTFE membranes (Millipore) using vacuum filtration. The film was allowed to settle for 15 minutes, rinsed with 30 mL DI water, and then dried in air. XPS measurements were performed promptly using a Thermo Scientific ESCALAB 250Xi. XPS spectra were corrected for background and fitted for peaks manually.[36]

Total organic carbon (TOC) was measured using a Shimadzu TOC-Vcsh total organic carbon analyzer with the NDIR method (combustion at 720 °C due to the attached total nitrogen measurement unit). The TOC analyzer is capable of detecting the total organic carbon concentration in the sample. Sample solutions were diluted and transferred to 40 mL vials. The

volume of injected solution was 80 μL, with three injections for each sample. After analyzing 10 samples, a wash was performed.

2.4 Statistical Analysis

Statistical testing was employed for data analysis. Two-sample t-tests for hypothesis testing were conducted using OriginPro 2016 software (OriginLab Corporation, MA) to guarantee the statistical significance of the conclusions. Probability values (P) of less than 0.05 were considered as statistically significant.

3. RESULTS AND DISCUSSION

3.1 Physicochemical Properties of GO and rGO

Table 1 shows the lateral size distributions based on the AFM images of the GO and rGO samples before and after irradiation. Before irradiation, the lateral sizes of all GO and rGO nanomaterials are similar, indicating that the reduction process does not change the physical dimensions of the GO or rGO flakes ($P > 0.05$). Hydrodynamic diameter measurements confirmed that there was no significant difference ($P > 0.05$) in particle size between the initial GO, rGO-2h, and rGO-5h dispersions (Table S1). However, sizes of rGO-2h, and rGO-5h are statistically different ($P < 0.05$), with rGO-5h having higher size. Zeta potential measurements, across all initial dispersions indicate stable dispersions due to electrostatic repulsion among particles (Table S2).

Initial XPS spectra of GO, rGO-2h, and rGO-5h are shown in Figure 3. The spectra exhibit three major peaks corresponding to C-C at 284.8 eV, epoxy and hydroxyl functional groups (C-O) at 286.9 eV, and carbonyl groups (C=O) at 289 eV.[39-41] These peaks were quantified and are listed in Table 2. During the solvothermal process, the epoxy and hydroxyl groups on the basal plane of the GO are driven off, evident by the decrease in the C-O peak and the overall decrease of oxygen in rGO-2h and rGO-5h ($P < 0.05$). Furthermore, the emergence of the peak at 292 eV, due to the $\pi \rightarrow \pi^*$ transition, is indicative of the restoration of the graphene lattice.

This composition data is further supported by the optical absorbance spectra of the GO nanomaterials. The initial GO dispersion shows absorption peaks at 230 nm, related to the π-π^* transitions of the aromatic C–C bonds, and a shoulder at 300 nm, corresponding to the n-π^* transitions due to the presence of oxygen containing functional groups, such as epoxide (C – O – C) (Figure 4a).[42-47] Conversely, the initial rGO-2h and rGO-5h dispersions show a single absorption peak at 270 nm, indicating the restoration of the π-conjugated network of graphene. Furthermore, the disappearance of the shoulder at 300 nm suggests the loss of oxygen-containing groups (Figure 4b, 4c). [48-52]

Overall, three GO dispersions were prepared wherein the surface oxidation was systematically varied while other material properties were kept constant to determine the role of oxygen-containing functional groups on the direct photolysis of graphene family nanomaterials.

3.2 Photodegradation of GO and rGO

3.2.1 AFM Analysis

The three GO nanomaterial dispersions were exposed to simulated sunlight, and the size of the particles was monitored using AFM. In Figure 1, AFM images of both rGO-2h and rGO-5h show no considerable change in the size of the particles after 24 h of irradiation. Detailed quantitative results from AFM images are presented in Table 1, showing no significant change ($P > 0.05$) in the size of rGO-2h and rGO-5h after 24 h of irradiation. On the other hand, GO particles reduced in lateral size from 180 ± 160 nm to 100 ± 50 nm (a reduction of ~ 44%) within the first 24 h of irradiation (Table 1). This reduction of size is immediately apparent in the AFM images (Figure 1). This rapid decrease in the lateral size of the GO indicates that the material is breaking down quickly upon irradiation while rGO degrades at a significantly slower rate.

3.2.2 TOC Analysis

Degradation of rGO and GO particles was further investigated by TOC measurements. Previously, reduction of organic carbon through oxidative photochemical degradation has been observed with other nanomaterials and pollutants in the presence of UV light and sunlight.[6, 53-55] GO samples showed a TOC reduction of 32.1% after 3 days of irradiation (Figure 2). It should be noted that the majority of this TOC reduction occurred in the first 6 hours (27.65%) but then slowed considerably over the next 162 hours, indicating that GO undergoes rapid photodegradation upon the initial 6 hours of exposure to sunlight. TOC reduction for rGO-2h and rGO-5h after 3 days of irradiation was 28.8% and 14.5%, respectively, which is a slower TOC reduction compared to GO ($P < 0.05$). Among rGO-2h and rGO-5h samples, the slowest rate of

TOC reduction was observed for rGO-5h ($P < 0.05$). These results further confirm the delayed degradation of rGO samples. A previous study of GO transformation by direct photolysis under simulated sunlight ,[31] with similar experimental conditions showed from mass spectrometry analysis that direct photolysis will rapidly remove GO by photochemically converting it to CO_2, fragmented photoproducts similar to rGO, and LMW species (mainly hydroxylated and/or carboxylated PAH compounds). The formation of oxygenated PAH species was consistent with previous work in which GO transformation was driven by a photo-Fenton reaction.[11, 12]

3.2.3 Electrokinetic and Hydrodynamic Properties of Phototransformed GO and rGO

A Zetasizer Nano ZS was used to analyze the change in particle size. From the hydrodynamic diameter values, a rapid decrease in the size of the GO (~ 36%) is observed compared to rGO-2h (~ 25%) and rGO-5h (~ 12%) after 24 h (Table S1; $P < 0.05$). Even after 48 h, size of GO decreases further (~ 45%) from the initial size. However, in exposure under prolonged light (168 h), GO material got decreased compared to its initial size, but this reduction is not that significant alike the size reduction in the initial exposure time. Major size reduction occurred during the initial hours of exposure to sunlight. [31] This decrease in size for GO was verified with the TOC analysis as well showed in Figure S3. On the other hand, extended light exposure promotes rGO aggregation, which leads to increase in size measurements. This size reduction is attributed to the degradation of graphene oxide flakes during irradiation, which is supported by the AFM analysis (Figure 1), implying that the rGO samples degrade at a significantly slower rate.

Zeta potential (ZP) is an important indicator of the stability of particles. ZP values of both GO and rGO samples were in the range of -30 to -50 mV (Table S2). From the negative value of the

ZP, it can be concluded that the particles have a negatively charged surface. Furthermore, the magnitude of the ZP indicates that all GO samples are stably dispersed.[56, 57] However, despite having a negative ZP of greater magnitude than 30 mV, rGO samples were found to be relatively unstable (Figure 5b, 5c), due to the lower amount of oxygen-containing functional groups and resulting higher hydrophobicity. [16, 58, 59]

3.2.4 Evolution of Functional Groups

Changes in the oxygen-containing functional groups as a result of the photodegradation were verified by XPS. Figure 3 and Table 2 summarize the chemical degradation of the GO nanomaterials. After 72 hours of irradiation, ~ 16% reduction of hydroxyl (C-OH) and epoxy (C-O-C) groups in the rGO materials are observed. GO, on the other hand, undergoes a noticeable chemical reduction where the amount of hydroxyl and epoxy groups decreases significantly from 39.7% to 13.9% (~ 65%) upon irradiation for 72 hours ($P < 0.05$) and the XPS spectrum of GO after photodegradation resembles that of rGO. These hydroxyl and epoxy functional groups are located primarily on the basal plane of graphene oxide, and it is hypothesized that these functional groups will react first in the presence of sunlight as they are single bonded groups. Functional groups on the edges, such as carboxylic acid, are much more stable and less likely to react initially. From XPS spectra, ratio of C=O increases indicating that COOH functional groups are more stable and relative fraction of COOH functional groups increases with photo-degradation. Changes in the oxygen-containing functional groups as a result of the photodegradation were also verified by UV-Vis optical absorbance spectroscopy. The presence of oxygen-containing functional groups on the surface disrupt the conjugated system of

graphene, causing a shift in the absorbance peaks.[51, 52] The samples were irradiated, and the absorbance at 400 nm was monitored over time (Figure S4). In the case of GO, the absorbance increased over time, indicating a photochemical change likely caused by the formation of light-absorbing photoproducts.[31] Sunlight exposure also resulted in a shift in the peak position from 230 nm to 270 nm, indicating the restoration of the π-conjugation network of graphene (Figure 4a). The disappearance of the shoulder at 300 nm suggests the removal of oxygen groups (such as hydroxyl and epoxy groups) consistent with the XPS results.[48-50] Conversely, no significant changes of UV-Vis spectra are observed in the rGO materials (Figure 4b, 4c).

Figure 5a shows that as the photodegradation progressed, the color of the GO samples darkened due to sunlight exposure, again indicative of degradation of GO. Previously,[60, 61] this color change has been observed and attributed to the partial restoration of the conjugated carbon ring network due to the removal of oxygen-containing functional groups. This same phenomenon has been observed during the chemical reduction of GO sheets, discussed earlier.[62, 63] Removal of these functional groups due to sunlight exposure would also result in the particles becoming more hydrophobic (Figure 5b, 5c). This increased hydrophobicity could induce aggregation in the rGO samples and delay the degradation of rGO-2h and rGO-5h. Moreover, beyond a certain irradiation time, rGO particles begin to form larger aggregates that can settle, reducing the opportunity for photodegradation of the material. Aggregation and settling characteristics of graphene nanomaterials observed in this study are consistent with previous studies with carbon nanotubes (CNTs) where it was observed that UVC irradiation destabilized a colloidal suspension of CNTs. In these studies,[24, 25] it was observed that removal of oxygen-containing functional groups decreased the electrostatic repulsion between particles and caused aggregation. However, no significant structural transformation was observed for the samples.[24, 25]

3.3 Kinetic analysis

For GO and rGO nanomaterials, the photolysis kinetics can be expressed by the following equation,

$$-\frac{d[A]}{dt} = k_{obs,A}[A]$$

Where $k_{obs,A}$ is the pseudo-first-order rate constant of direct photolysis of compound A (A = GO or rGO-2h or rGO-5h). Degradation kinetics of GO occurs in two (fast and slow) stages. For GO nanomaterials, the loss or degradation of material, which is measured as the decrease in TOC concentration (Figure S5), occurs in two (fast and slow) stages. The fastest degradation occurs during the initial exposure to sunlight (first 24 h) in which $k_{obs,GO}$ was determined to be 0.017 h^{-1} (R^2 = 0.91). After 24 h of sunlight exposure, the loss of nanomaterial was slower, and $k_{obs,GO}$ was determined to be 0.007 h^{-1} (R^2 = 0.80) after 72 h of sunlight exposure. So, two-stage kinetics has been observed in the photo-degradation of GO (Figure S5). Initially, rate was high, and pseudo-first order kinetics were observed; then, in the second phase, degradation became slower. [64]

The $k_{obs,rGO-2h}$ slightly decreased to 0.005 h^{-1} (R^2 = 0.83), in comparison to $k_{obs,GO}$ while $k_{obs,rGO-5h}$ significantly decreased to 0.002 h^{-1} (R^2 = 0.51), in comparison to $k_{obs,rGO-2h}$ (Figure S5). As the pseudo-first-order rate constants for rGO-2h and rGO-5h are less than that of GO, it indicates that TOC decrease is higher for GO, compared to rGO materials. Hence, the order of degradation rate follows GO > rGO-2h > rGO-5h.

3.4 Proposed Mechanisms

Figure 6 shows the proposed mechanisms for the photodegradation of GO and rGO under direct sunlight. In direct photolysis, functional groups of graphene nanomaterials act as chromophores.[31, 65-67] Hydroxyl and epoxy functional groups, located mainly on the basal plane

of GO, are hypothesized to react first in the presence of sunlight as they are single bonded groups. Other functional groups on the edges are double bonded groups, which require more energy to break than single bonds, and are thus less likely to react initially.[68, 69]

The hydroxyl and epoxy functional groups (C-OH and C-O), which are strong electron donating groups, absorb photons that excite electrons from the ground state to the excited state, producing many excited electrons and holes.[70] Eventually, these electrons and holes disrupt the chemical bonds of the functional groups, initiating the breaking of the covalent bonds and contributing to the physical breakdown of the GO material.[70-74]

GO, consists of insulating or semi-conducting sp^3-hybridized carbon domains on the basal plane and non-oxidized sp^2 segments that are either aromatic or conjugated. [75] During photo-reduction, the bandgap excitation of the semiconducting region is responsible for reduction process. [76] A typical semiconductor has an energy gap between the valence and conduction band. On exposure to the visible light, GO absorbs photons of energy equal to or larger than its bandgap to excite an electron from the valence band into the conduction band. Therefore, creating an electron in the conduction band and empty energy state in the valence band- the hole. [77, 78] These electrons and holes contribute to the redox reactions on GO sheet.

C-O has a bond energy of 358 kJ/mol or 5.945×10^{-19} J/photon (Note: The Avogadro constant, has the value 6.022×10^{23} mol^{-1}).

The energy associated with radiation is given by

$$E = \frac{hc}{\lambda}$$

Where,

E is the energy in Joules,

h is Planck's constant ($h = 6.626 \times 10^{-34}$ J s),

c is the speed of light, ($c = 3.0 \times 10^{8}$ m s^{-1}) and

λ is wavelength of light in units of nm.

To break the oxygen containing bond (C-O and C-OH), the required wavelength calculated from the above equation is 335 nm, which is well within the range of our applied irradiation (300 nm to 800 nm). This quantitatively proves the breakup of the oxygen containing functional groups from the basal plane of GO material.

Other functional groups, remaining on the edge will not react initially as they are double bonded groups, which requires more energy to break (C=O: 745 kJ/mol or 1.237×10^{-18} J/photon, requiring 160 nm wavelength).[68, 69, 79]

rGO has significantly fewer oxygen-containing functional groups than GO. Specifically, the amount of hydroxyl and epoxy functional groups is significantly lower (Table 2). This reduction in electron donating functional groups in rGO will reduce the breaking of covalent bonds in rGO. Hence, rGO is more resistant to degradation than GO under direct photolysis, as we have shown in our photodegradation studies. Furthermore, rGO particles aggregate due to the increased hydrophobicity of these materials, which can reduce the opportunity for photodegradation. Aqueous aggregation (stability) of nanomaterials significantly impacts effective toxicity, environmental transport, and ultimate material fate. [80] Moreover, aggregation can alter

nanoparticle reactivity, and nanoparticle aggregation state can be altered by photochemical environmental processes. [81] Reduced content of functional groups increases hydrophobicity of rGO particles. As rGO becomes more hydrophobic, it becomes more prone to form aggregates (i.e. increase in size) and less prone to degrade. So, both reactivity and stability (aggregation) play roles in the degradation.

3.4.a. Degradation Analysis with Density Functional Theory (DFT)

We further used DFT method to characterize the thermodynamic energy change for the structure degradation of GO sheets. We assumed that the degradation process consists of two consecutive steps: 1) removal of functional groups on graphene plane; and 2) C-C bond breakage. The DFT calculations were performed using the ADF software. [82] Two types of GO models were considered: one has single hydroxyl group (denoted as GO1, which is rGO) and another one has two hydroxyl groups (denoted as GO2, which is GO). All initial structures were optimized and single-point energy calculations were performed by the B3LYP-D3/TZP method.

From our computation (Figure 7a), in the first step, the removal of one hydroxyl functional group is kinetics process with an existence of transition state (TS). However, in the second step, the breakage of C-C bond is thermodynamic unfavorable process with energetic penalty. For GO2, corresponding to higher oxidation degree, the barrier of transition state is very small (~0.6 kcal/mol), however, the energy barrier to remove hydroxyl group for GO1 is ~6.0 kcal/mol, which is obviously larger than that of GO2. We further calculated the energy profiles for the assumed GO degradation process with the C-C breakage, wherein there are breakage of three C-C bonds. As shown in Figure 7b, the required energy of breaking C-C bond in the GO1 structure is to some extent higher than that of GO2, showing that the

degradation of GO with lower oxidation degree, which is GO1 (rGO), is more difficult. It should be noted that the energy difference is relatively minor, possibly due to small size of graphene model with only 1-2 hydroxyl groups. However, this different energetic profiles indeed support that the experimental conclusion that more degradation of GO sheets with higher oxidization degree can be realized.

Overall, these results suggest that sunlight exposure causes significant degradation of graphene oxide, but no significant change in reduced graphene oxide nanomaterials is observed. Oxygen-containing functional groups on the basal plane, are the most likely photoreactive sites that contribute to the breakdown of GO nanomaterials.[83-85] The presence of fewer oxygen-containing functional groups on the surface of rGO materials leads to delayed degradation of the material.

4. ENVIRONMENTAL IMPLICATIONS

Collective results from this study indicate that the surface oxidation of graphene nanomaterials strongly affects sunlight-induced photolysis. The oxygen-containing functional groups, primarily those present on the basal plane, play a strong role in the photodegradation of GO. This degradation will have an obvious impact on the fate of these emerging materials in the environment. Based on the findings of this research, it can be assumed that graphene oxide nanomaterials will undergo degradation in natural surface water due to sunlight exposure, which potentially leads to nanoparticle release into the environment. Since nanoparticles have shown potential risks to human health and environment, their release during the life cycle could restrain commercialization of these nanomaterials. In particular, graphene oxide nanomaterials with higher levels of oxidation will experience higher rates of photodegradation, while reduced forms

of graphene oxide will show a higher resistance to this degradation due to fewer functional groups on the surface. These findings will also be helpful for designing sustainable graphene nanomaterials for various applications. For coatings and photocatalytic applications, graphene nanomaterials are desired to be resistant to photodegradation. Hence, graphene with lower amount of oxygen containing functional groups will be useful for coatings and photocatalytic applications.

ACKNOWLEDGMENTS

This work was supported by US Geological Survey grant (2016WA411B) via State of Washington Water Research Center**.** The sample preparation and characterization at Northwestern University was supported by the National Science Foundation and the Environmental Protection Agency under Cooperative Agreement Number DBI-1266377.

Supporting Information.

Additional details on materials, methods and results are available in Supporting Information.

REFERENCES

1. K. S. Novoselov, V. I. Fal'ko, L. Colombo, P. R. Gellert, M. G. Schwab and K. Kim, A roadmap for graphene, *Nature*, 2012, **490**, 192.
2. K. C. Kemp, H. Seema, M. Saleh, N. H. Le, K. Mahesh, V. Chandra and K. S. Kim, Environmental applications using graphene composites: water remediation and gas adsorption, *Nanoscale*, 2013, **5**, 3149-3171.
3. C. Chung, Y.-K. Kim, D. Shin, S.-R. Ryoo, B. H. Hong and D.-H. Min, Biomedical Applications of Graphene and Graphene Oxide, *Accounts of Chemical Research*, 2013, **46**, 2211-2224.
4. C. Cheng, J. Zhang, S. Li, Y. Xia, C. Nie, Z. Shi, J. L. Cuellar-Camacho, N. Ma and R. Haag, A Water-Processable and Bioactive Multivalent Graphene Nanoink for Highly Flexible Bioelectronic Films and Nanofibers, *Advanced Materials*, 2018, **30**, 1705452.
5. C. He, Z.-Q. Shi, C. Cheng, H.-Q. Lu, M. Zhou, S.-D. Sun and C.-S. Zhao, Graphene oxide and sulfonated polyanion co-doped hydrogel films for dual-layered membranes with superior hemocompatibility and antibacterial activity, *Biomaterials science*, 2016, **4**, 1431-1440.
6. N. Savage and M. S. Diallo, Nanomaterials and water purification: opportunities and challenges, *Journal of Nanoparticle research*, 2005, **7**, 331-342.
7. M. Aliofkhazraei, N. Ali, W. I. Milne, C. S. Ozkan, S. Mitura and J. L. Gervasoni, *Graphene Science Handbook: Electrical and Optical Properties*, CRC Press, 2016.
8. A. K. Geim, Graphene: status and prospects, *Science*, 2009, **324**, 1530.
9. D. R. Dreyer, S. Park, C. W. Bielawski and R. S. Ruoff, The chemistry of graphene oxide, *Chem. Soc. Rev.*, 2010, **39**, 228.
10. T. Nakato, J. Kawamata and S. Takagi, *Inorganic Nanosheets and Nanosheet-Based Materials: Fundamentals and Applications of Two-Dimensional Systems*, Springer Japan, 2017.

11. H. Bai, W. Jiang, G. P. Kotchey, W. A. Saidi, B. J. Bythell, J. M. Jarvis, A. G. Marshall, R. A. S. Robinson and A. Star, Insight into the Mechanism of Graphene Oxide Degradation via the Photo-Fenton Reaction, *J. Phys. Chem. C*, 2014, **118**, 10519.

12. X. Zhou, Y. Zhang, C. Wang, X. Wu, Y. Yang, B. Zheng, H. Wu, S. Guo and J. Zhang, Photo-Fenton Reaction of Graphene Oxide: A New Strategy to Prepare Graphene Quantum Dots for DNA Cleavage, *ACS Nano*, 2012, **6**, 6592.

13. G. Mastrangelo, E. Fadda and V. Marzia, Polycyclic aromatic hydrocarbons and cancer in man, *Occupational Health and Industrial Medicine*, 1997, **3**, 113.

14. Y. Feng, K. Lu, L. Mao, X. Guo, S. Gao and E. J. Petersen, Degradation of 14C-labeled few layer graphene via Fenton reaction: Reaction rates, characterization of reaction products, and potential ecological effects, *Water research*, 2015, **84**, 49-57.

15. G. Wang, F. Qian, C. W. Saltikov, Y. Jiao and Y. Li, Microbial reduction of graphene oxide by Shewanella, *Nano Research*, 2011, **4**, 563-570.

16. X. Ren, J. Li, C. Chen, Y. Gao, D. Chen, M. Su, A. Alsaedi and T. Hayat, Graphene analogues in aquatic environments and porous media: dispersion, aggregation, deposition and transformation, *Environmental Science: Nano*, 2018, **5**, 1298-1340.

17. I. Chowdhury, M. C. Duch, N. D. Mansukhani, M. C. Hersam and D. Bouchard, Colloidal Properties and Stability of Graphene Oxide Nanomaterials in the Aquatic Environment, *Environmental Science & Technology*, 2013, **47**, 6288-6296.

18. L. Wu, L. Liu, B. Gao, R. Muñoz-Carpena, M. Zhang, H. Chen, Z. Zhou and H. Wang, Aggregation Kinetics of Graphene Oxides in Aqueous Solutions: Experiments, Mechanisms, and Modeling, *Langmuir*, 2013, **29**, 15174.

19. W.-C. Hou and C. T. Jafvert, Photochemistry of Aqueous C60 Clusters: Evidence of 1O2 Formation and its Role in Mediating C60 Phototransformation, *Environmental Science & Technology*, 2009, **43**, 5257-5262.

20. W. C. Hou and C. T. Jafvert, Photochemical transformation of aqueous C60 clusters in sunlight, *Environ. Sci. Technol.*, 2009, **43**, 362.

21. W.-C. Hou, L. Kong, K. A. Wepasnick, R. G. Zepp, D. H. Fairbrother and C. T. Jafvert, Photochemistry of Aqueous C60 Clusters: Wavelength Dependency and Product Characterization, *Environmental Science & Technology*, 2010, **44**, 8121-8127.

22. L. Kong, O. Tedrow, Y. F. Chan and R. G. Zepp, Light-initiated transformations of fullerenol in aqueous media, *Environ. Sci. Technol.*, 2009, **43**, 9155.

23. Y. S. Hwang and Q. L. Li, Characterizing photochemical transformation of aqueous nC60 under environmentally relevant conditions, *Environ. Sci. Technol.*, 2010, **44**, 3008.

24. J. L. Bitter, J. Yang, S. Beigzadeh Milani, C. T. Jafvert and D. H. Fairbrother, Transformations of oxidized multiwalled carbon nanotubes exposed to UVC (254 nm) irradiation, *Environmental Science: Nano*, 2014, **1**, 324-337.

25. C.-Y. Chen and C. T. Jafvert, Photoreactivity of Carboxylated Single-Walled Carbon Nanotubes in Sunlight: Reactive Oxygen Species Production in Water, *Environmental Science & Technology*, 2010, **44**, 6674-6679.

26. C.-Y. Chen and R. G. Zepp, Probing Photosensitization by Functionalized Carbon Nanotubes, *Environmental Science & Technology*, 2015, **49**, 13835-13843.

27. W.-C. Hou, C.-J. He, Y.-S. Wang, D. K. Wang and R. G. Zepp, Phototransformation-Induced Aggregation of Functionalized Single-Walled Carbon Nanotubes: The Importance of Amorphous Carbon, *Environmental Science & Technology*, 2016, **50**, 3494-3502.

28. R. Y. N. Gengler, D. S. Badali, D. Zhang, K. Dimos, K. Spyrou, D. Gournis and R. J. D. Miller, Revealing the ultrafast process behind the photoreduction of graphene oxide, *Nature Communications*, 2013, **4**, 2560.

29. M. Koinuma, C. Ogata, Y. Kamei, K. Hatakeyama, H. Tateishi, Y. Watanabe, T. Taniguchi, K. Gezuhara, S. Hayami, A. Funatsu, M. Sakata, Y. Kuwahara, S. Kurihara and Y. Matsumoto,

Photochemical Engineering of Graphene Oxide Nanosheets, *The Journal of Physical Chemistry C*, 2012, **116**, 19822-19827.

30. Y. Matsumoto, M. Koinuma, S. Ida, S. Hayami, T. Taniguchi, K. Hatakeyama, H. Tateishi, Y. Watanabe and S. Amano, Photoreaction of Graphene Oxide Nanosheets in Water, *The Journal of Physical Chemistry C*, 2011, **115**, 19280-19286.

31. W.-C. Hou, I. Chowdhury, D. G. Goodwin, W. M. Henderson, D. H. Fairbrother, D. Bouchard and R. G. Zepp, Photochemical Transformation of Graphene Oxide in Sunlight, *Environmental Science & Technology*, 2015, **49**, 3435-3443.

32. G. P. Kotchey, B. L. Allen, H. Vedala, N. Yanamala, A. A. Kapralov, Y. Y. Tyurina, J. Klein-Seetharaman, V. E. Kagan and A. Star, The Enzymatic Oxidation of Graphene Oxide, *ACS Nano*, 2011, **5**, 2098-2108.

33. H. Bai, W. Jiang, G. P. Kotchey, W. A. Saidi, B. J. Bythell, J. M. Jarvis, A. G. Marshall, R. A. S. Robinson and A. Star, Insight into the Mechanism of Graphene Oxide Degradation via the Photo-Fenton Reaction, *The Journal of Physical Chemistry C*, 2014, **118**, 10519-10529.

34. G. E. Batley, J. K. Kirby and M. J. McLaughlin, Fate and Risks of Nanomaterials in Aquatic and Terrestrial Environments, *Accounts of Chemical Research*, 2013, **46**, 854-862.

35. N. I. Kovtyukhova, P. J. Ollivier, B. R. Martin, T. E. Mallouk, S. A. Chizhik, E. V. Buzaneva and A. D. Gorchinskiy, Layer-by-layer assembly of ultrathin composite films from micron-sized graphite oxide sheets and polycations, *Chemistry of Materials*, 1999, **11**, 771-778.

36. I. Chowdhury, N. D. Mansukhani, L. M. Guiney, M. C. Hersam and D. Bouchard, Aggregation and Stability of Reduced Graphene Oxide: Complex Roles of Divalent Cations, pH, and Natural Organic Matter, *Environmental Science & Technology*, 2015, **49**, 10886-10893.

37. D. W. Johnson, B. P. Dobson and K. S. Coleman, A manufacturing perspective on graphene dispersions, *Current Opinion in Colloid & Interface Science*, 2015, **20**, 367-382.

38. Y. Su, G. Yang, K. Lu, E. J. Petersen and L. Mao, Colloidal properties and stability of aqueous suspensions of few-layer graphene: Importance of graphene concentration, *Environmental Pollution*, 2017, **220**, 469-477.

39. S. Stankovich, D. A. Dikin, R. D. Piner, K. A. Kohlhaas, A. Kleinhammes, Y. Jia, Y. Wu, S. T. Nguyen and R. S. Ruoff, Synthesis of graphene-based nanosheets via chemical reduction of exfoliated graphite oxide, *Carbon*, 2007, **45**, 1558.

40. L. J. Cote, F. Kim and J. Huang, Flash Reduction and Patterning of Graphite Oxide and Its Polymer Composite, *J. Am. Chem. Soc.*, 2009, **131**, 1043.

41. S. J. An, Y. Zhu, S. H. Lee, M. D. Stoller, T. Emilsson, S. Park, A. Velamakanni, J. An and R. S. Ruoff, Thin film fabrication and simultaneous anodic reduction of deposited graphene oxide platelets by electrophoretic deposition, *The Journal of Physical Chemistry Letters*, 2010, **1**, 1259-1263.

42. N. M. Huang, H. N. Lim, C. H. Chia, M. A. Yarmo and M. R. Muhamad, Simple room-temperature preparation of high-yield large-area graphene oxide, *International journal of nanomedicine*, 2011, **6**, 3443-3448.

43. Q. Mei, K. Zhang, G. Guan, B. Liu, S. Wang and Z. Zhang, Highly efficient photoluminescent graphene oxide with tunable surface properties, *Chemical Communications*, 2010, **46**, 7319-7321.

44. D. Li, M. B. Muller, S. Gilje, R. B. Kaner and G. G. Wallace, Processable aqueous dispersions of graphene nanosheets, *Nat Nano*, 2008, **3**, 101-105.

45. D. C. Marcano, D. V. Kosynkin, J. M. Berlin, A. Sinitskii, Z. Sun, A. Slesarev, L. B. Alemany, W. Lu and J. M. Tour, Improved synthesis of graphene oxide, *ACS Nano*, 2010, **4**, 4806.

46. X. Gao, J. Jang and S. Nagase, Hydrazine and Thermal Reduction of Graphene Oxide: Reaction Mechanisms, Product Structures, and Reaction Design, *The Journal of Physical Chemistry C*, 2010, **114**, 832-842.

47. S. Saxena, T. Tyson, S. Shukla, E. Negusse, H. Chen and J. Bai, *Investigation of structural and electronic properties of graphene oxide*, 2011.

48. K. Liu, J.-J. Zhang, F.-F. Cheng, T.-T. Zheng, C. Wang and J.-J. Zhu, Green and facile synthesis of highly biocompatible graphene nanosheets and its application for cellular imaging and drug delivery, *Journal of Materials Chemistry*, 2011, **21**, 12034-12040.

49. Y. Han, Z. Luo, L. Yuwen, J. Tian, X. Zhu and L. Wang, Synthesis of silver nanoparticles on reduced graphene oxide under microwave irradiation with starch as an ideal reductant and stabilizer, *Applied Surface Science*, 2013, **266**, 188-193.

50. Y. Zhou, Q. Bao, L. A. L. Tang, Y. Zhong and K. P. Loh, Hydrothermal Dehydration for the "Green" Reduction of Exfoliated Graphene Oxide to Graphene and Demonstration of Tunable Optical Limiting Properties, *Chemistry of Materials*, 2009, **21**, 2950-2956.

51. M. Sugioka, The Relationship Between UV-VIS Absorption and Structure of Organic Compounds, *UV Talk Letter February. Shimadzu*, 2009, **2**, 5-6.

52. M. Nakahara, The science of color.*Journal*, 2002.

53. N. Chitose, S. Ueta, S. Seino and T. A. Yamamoto, Radiolysis of aqueous phenol solutions with nanoparticles. 1. Phenol degradation and TOC removal in solutions containing TiO 2 induced by UV, γ-ray and electron beams, *Chemosphere*, 2003, **50**, 1007-1013.

54. K. Kabra, R. Chaudhary and R. L. Sawhney, Treatment of hazardous organic and inorganic compounds through aqueous-phase photocatalysis: a review, *Industrial & engineering chemistry research*, 2004, **43**, 7683-7696.

55. G. R. Malpass, D. W. Miwa, R. L. Santos, E. M. Vieira and A. J. Motheo, Unexpected toxicity decrease during photoelectrochemical degradation of atrazine with NaCl, *Environmental chemistry letters*, 2012, **10**, 177-182.

56. D. Li, M. B. Mueller, S. Gilje, R. B. Kaner and G. G. Wallace, Processable aqueous dispersions of graphene nanosheets, *Nat. Nanotechnol.*, 2008, **3**, 101.

57. Y. Si and E. T. Samulski, Synthesis of water soluble graphene, *Nano Lett.*, 2008, **8**, 1679-1682.

58. T. Xia, J. D. Fortner, D. Zhu, Z. Qi and W. Chen, Transport of sulfide-reduced graphene oxide in saturated quartz sand: Cation-dependent retention mechanisms, *Environmental science & technology*, 2015, **49**, 11468-11475.

59. Y. Qi, T. Xia, Y. Li, L. Duan and W. Chen, Colloidal stability of reduced graphene oxide materials prepared using different reducing agents, *Environmental Science: Nano*, 2016, **3**, 1062-1071.

60. D. Hou, Q. Liu, X. Wang, Y. Quan, Z. Qiao, L. Yu and S. Ding, Facile synthesis of graphene via reduction of graphene oxide by artemisinin in ethanol, *Journal of Materiomics*, 2018.

61. T. F. Emiru and D. W. Ayele, Controlled synthesis, characterization and reduction of graphene oxide: A convenient method for large scale production, *Egyptian Journal of Basic and Applied Sciences*, 2017, **4**, 74-79.

62. H. A. Becerril, J. Mao, Z. Liu, R. M. Stoltenberg, Z. Bao and Y. Chen, Evaluation of Solution-Processed Reduced Graphene Oxide Films as Transparent Conductors, *ACS Nano*, 2008, **2**, 463.

63. N. A. Kotov, I. Dekany and J. H. Fendler, Ultrathin Graphite Oxide-Polyelectrolyte Composites Prepared by Self-Assembly: Transition Between Conductive and NonConductive States, *Adv. Mater.*, 1996, **8**, 637.

64. M. Minella, M. Demontis, M. Sarro, F. Sordello, P. Calza and C. Minero, Photochemical stability and reactivity of graphene oxide, *Journal of materials science*, 2015, **50**, 2399-2409.

65. G. V. Lowry, K. B. Gregory, S. C. Apte and J. R. Lead, Transformations of nanomaterials in the environment.*Journal*, 2012.

66. W.-C. Hou and C. T. Jafvert, Photochemical transformation of aqueous C60 clusters in sunlight, *Environmental science & technology*, 2008, **43**, 362-367.

67. C.-Y. Chen and C. T. Jafvert, The role of surface functionalization in the solar light-induced production of reactive oxygen species by single-walled carbon nanotubes in water, *Carbon*, 2011, **49**, 5099-5106.

68. G. n. r. Gündüz, *Chemistry, materials, and properties of surface coatings : traditional and evolving technologies*, DEStech Publications, Lancaster, Pennsylvania :, 2016.

69. J. Robert C. Neuman, 1992-2013, ch. 1.

70. M. Mohandoss, S. S. Gupta, A. Nelleri, T. Pradeep and S. M. Maliyekkal, Solar mediated reduction of graphene oxide, *RSC Advances*, 2017, **7**, 957-963.

71. T. Mill, W. Mabey, B. Lan and A. Baraze, Photolysis of polycyclic aromatic hydrocarbons in water, *Chemosphere*, 1981, **10**, 1281-1290.

72. M. P. Fasnacht and N. V. Blough, Aqueous photodegradation of polycyclic aromatic hydrocarbons, *Environmental science & technology*, 2002, **36**, 4364-4369.

73. M. P. Fasnacht and N. V. Blough, Mechanisms of the aqueous photodegradation of polycyclic aromatic hydrocarbons, *Environmental Science & Technology*, 2003, **37**, 5767-5772.

74. R. G. Zepp and P. Schlotzhauer, Photoreactivity of selected aromatic hydrocarbons in water, *Polynuclear aromatic hydrocarbons*, 1979, 141-158.

75. A. Lerf, H. He, M. Forster and J. Klinowski, Structure of Graphite Oxide Revisited, *J. Phys. Chem. B*, 1998, **102**, 4477.

76. B. Konkena and S. Vasudevan, Engineering a Water-Dispersible, Conducting, Photoreduced Graphene Oxide, *The Journal of Physical Chemistry C*, 2015, **119**, 6356-6362.

77. J. Liu, M. Durstock and L. Dai, Graphene oxide derivatives as hole-and electron-extraction layers for high-performance polymer solar cells, *Energy & Environmental Science*, 2014, **7**, 1297-1306.

78. I. Kotin, I. Antonova, O. Orlov and S. Smagulova, Origin of hole and electron traps in graphene oxide, *Materials Research Express*, 2016, **3**, 066301.

79. D. J. Goss and R. H. Petrucci, *General Chemistry Principles & Modern Applications, Petrucci, Harwood, Herring, Madura: Study Guide*, Pearson/Prentice Hall, 2007.

80. Y. Jiang, R. Raliya, P. Liao, P. Biswas and J. D. Fortner, Graphene oxides in water: assessing stability as a function of material and natural organic matter properties, *Environmental Science: Nano*, 2017, **4**, 1484-1493.

81. E. M. Hotze, T. Phenrat and G. V. Lowry, Nanoparticle Aggregation: Challenges to Understanding Transport and Reactivity in the Environment, *J. Environ. Qual.*, 2010, **39**, 1909.

82. G. t. Te Velde, F. M. Bickelhaupt, E. J. Baerends, C. Fonseca Guerra, S. J. van Gisbergen, J. G. Snijders and T. Ziegler, Chemistry with ADF, *Journal of Computational Chemistry*, 2001, **22**, 931-967.

83. X. Zheng, Y. Peng, Y. Yang, J. Chen, H. Tian, X. Cui and W. Zheng, Hydrothermal reduction of graphene oxide; effect on surface-enhanced Raman scattering, *Journal of Raman Spectroscopy*, 2017, **48**, 97-103.

84. X. Mei, X. Meng and F. Wu, Hydrothermal method for the production of reduced graphene oxide, *Physica E: Low-dimensional Systems and Nanostructures*, 2015, **68**, 81-86.

85. X. Fan, W. Peng, Y. Li, X. Li, S. Wang, G. Zhang and F. Zhang, Deoxygenation of exfoliated graphite oxide under alkaline conditions: a green route to graphene preparation, *Advanced Materials*, 2008, **20**, 4490-4493.

List of Figures

Figure 1 AFM images of GO (top), rGO-2h (middle), and rGO-5h (bottom) showing size distributions of the particles before and after irradiation. After 24 h of sunlight exposure, GO degrades into smaller flakes while rGO shows no significant change in particle size.

Figure 2 Total organic carbon analysis of GO, rGO-2h, and rGO-5h samples in direct photolysis over 3 days. Highest TOC reduction is observed for GO while the smallest change in TOC is observed for rGO-5h. (Error bars indicate one standard deviation of at least three samples)

Figure 3 XPS spectra of the C 1s region for (a) GO (0 h), (b) GO (72 h), (c) rGO-2h (0 h), (d) rGO-2h (72 h), (e) rGO-5h (0 h), and (f) rGO-5h (72 h). GO undergoes a noticeable chemical reduction where the amount of hydroxyl (C-OH) and epoxy (C-O-C) groups decreases significantly upon irradiation for 72 hours, while no significant compositional changes in the rGO materials are observed.

Figure 4 Optical absorbance spectra of irradiated (a) GO, (b) rGO-2h, (c) rGO-5h samples. The shift in the major peak from 230 nm to 270 nm in GO implies the restoration of the graphene lattice, and the disappearance of the peak at 300 nm indicates the removal of oxygen-containing functional groups in GO. No significant changes are observed in the optical absorbance spectra for the rGO materials after irradiation.

Figure 5 Photographs of (a) GO, (b) rGO-2h, and (c) rGO-5h dispersions before (0 h) and after (72 h) sunlight exposure. The darkened color of the GO dispersion after 72 h of sunlight exposure is indicative of chemical and physical degradation. In contrast, the more hydrophobic rGO materials form aggregates in water, reducing the opportunity for photodegradation.

Figure 6 Schematics of the proposed reaction pathway for graphene oxide nanomaterial degradation. Above, GO is shown with oxygen-containing (hydroxyl and epoxy) functional groups. Due to absorption of photons from sunlight, the functional groups are removed, accelerating the physical degradation. Below, rGO with fewer functional groups, undergoes reduced degradation than GO under similar irradiation.

Figure 7. Energetic profiles of the structure degradation for GO (denoted as GO2) and rGO (denoted as GO1) with various oxidization degrees.（a） Potential energy surface plots for the removal of hydroxyl group from GO1 and GO2, respectively. (b) Potential energy curve for the breakage of three C-C bonds in three consecutive steps.Here, O, red; H, white; C on GO1 and GO2 is green and gray, respectively.

List of Tables

Table 1 Lateral size distributions of the GO and rGO nanomaterials based on AFM imaging (n= 70-247 flakes for GO and n = 10-20 flakes for rGO-2h and rGO-5h. For the rGO-2h and rGO-5h, since these materials aggregate, it is difficult to find individual flakes via AFM; uncertainties always indicate standard deviation values if not specified)

Table 2 Compositional details of the GO and rGO nanomaterials based on the XPS C 1s spectra (n = 5 scans)

Tables

Table 1 Lateral size distributions of the GO and rGO nanomaterials based on AFM imaging (n= 70-247 flakes for GO and n = 10-20 flakes for rGO-2h and rGO-5h. For the rGO-2h and rGO-5h, since these materials aggregate, it is difficult to find individual flakes via AFM; uncertainties always indicate standard deviation values if not specified)

Sample	**Lateral Size (nm)**	
	0 h	**24 h**
GO	180 ± 160	100 ± 50
rGO-2h	190 ± 150	210 ± 140
rGO-5h	160 ± 110	170 ± 110

Table 2 Compositional details of the GO and rGO nanomaterials based on the XPS C 1s spectra (n = 5 scans)

	GO		rGO-2h		rGO-5h	
	0 h	**72 h**	**0 h**	**72 h**	**0 h**	**72 h**
C-C	24.4 ± 1.6	47.4 ± 0.1	43.6 ± 0.5	49.2 ± 0.2	51.6 ± 0.6	47.4 ± 0.1
C-O	39.7 ± 0.9	13.9 ± 0.1	27.2 ± 1.1	22.7 ± 1.7	15.9 ± 0.7	21.6 ± 0.3
C=O	3.1 ± 0.2	12.1 ± 0.1	5.2 ± 0.7	5.6 ± 1.5	10.5 ± 1.5	7.2 ± 0.4
π→π*	-	3.3 ± 0.1	2.4 ± 0.1	4.4 ± 0.1	8.3 ± 0.1	9.7 ± 0.1
Oxygen	32.8 ± 0.4	23.4 ± 0.1	21.6 ± 0.1	18.0 ± 0.1	13.7 ± 0.1	14.1 ± 0.1

Figures

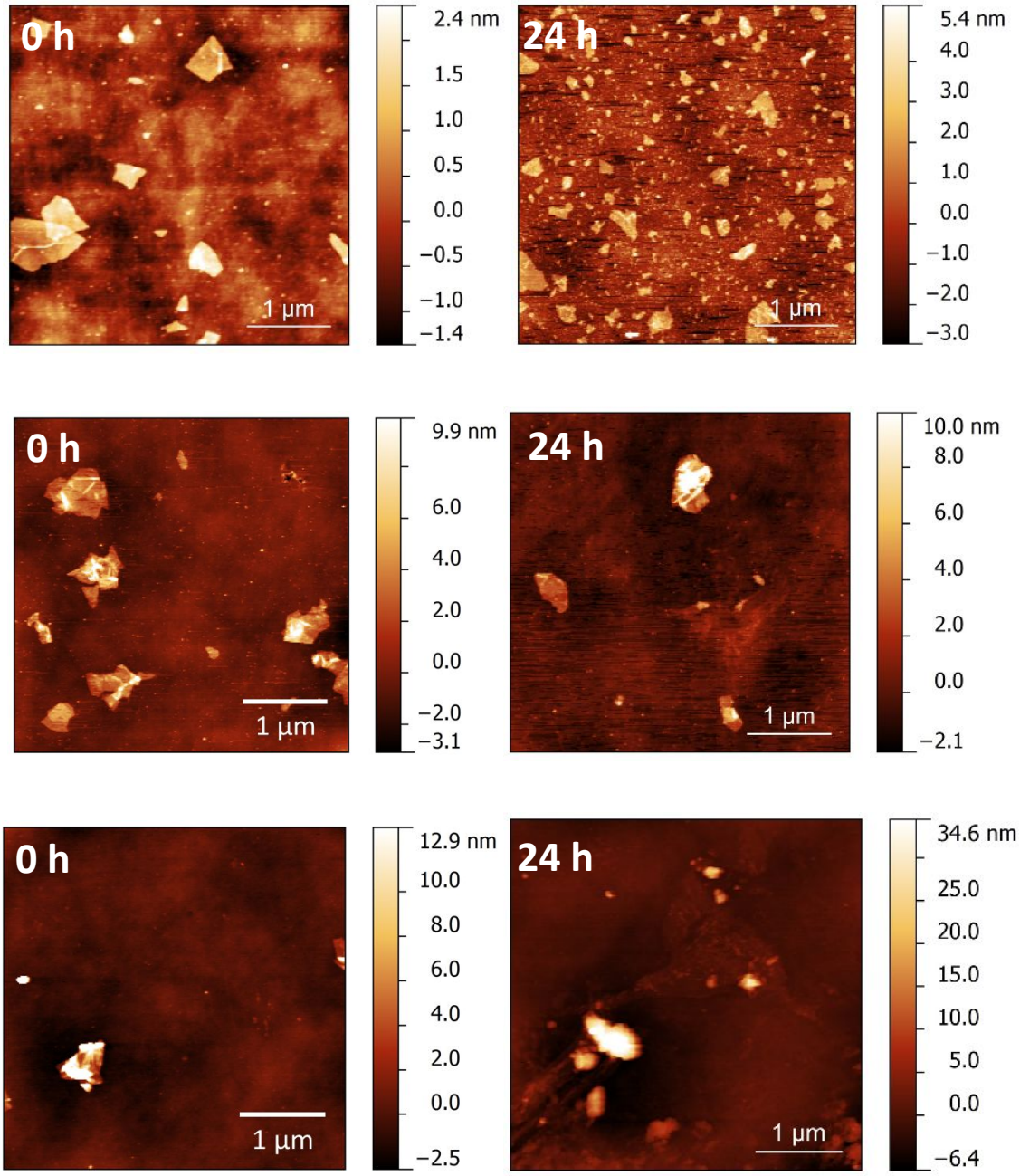

Figure 1. AFM images of GO (top), rGO-2h (middle), and rGO-5h (bottom) showing size distributions of the particles before and after irradiation. After 24 h of sunlight exposure, GO degrades into smaller flakes while rGO shows no significant change in particle size.

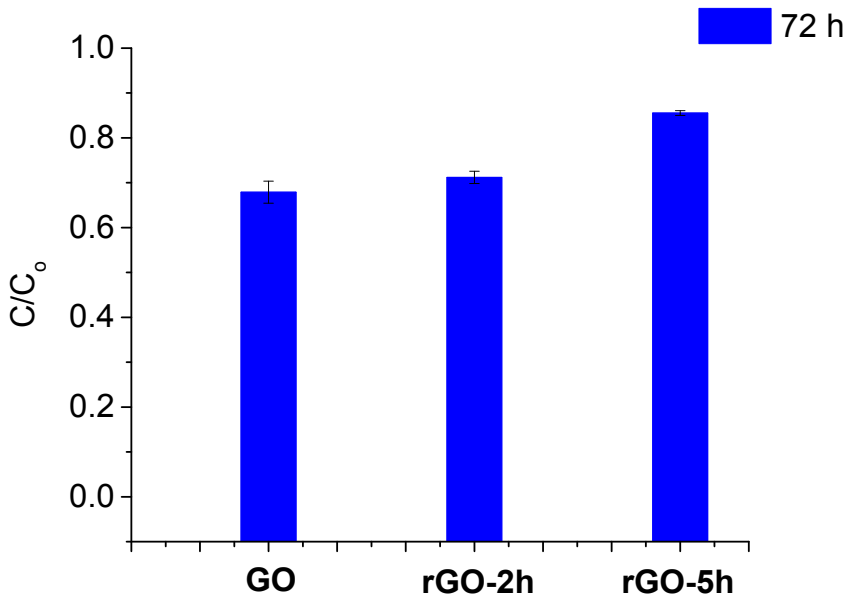

Figure 2. Total organic carbon analysis of GO, rGO-2h, and rGO-5h samples in direct photolysis over 3 days. Highest TOC reduction is observed for GO while the smallest change in TOC is observed for rGO-5h. (Error bars indicate one standard deviation of at least three samples)

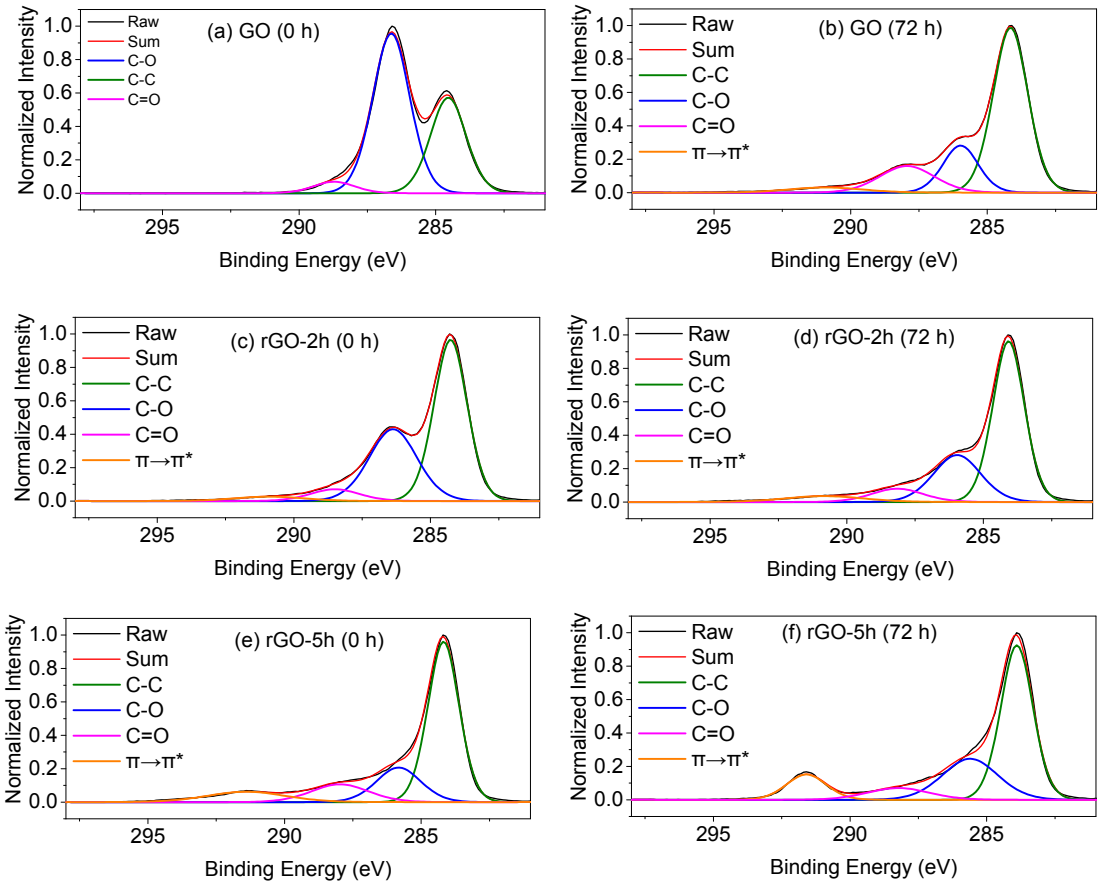

Figure 3. XPS spectra of the C 1s region for (a) GO (0 h), (b) GO (72 h), (c) rGO-2h (0 h), (d) rGO-2h (72 h), (e) rGO-5h (0 h), and (f) rGO-5h (72 h). GO undergoes a noticeable chemical reduction where the amount of hydroxyl (C-OH) and epoxy (C-O-C) groups decreases significantly upon irradiation for 72 hours, while no significant compositional changes in the rGO materials are observed.

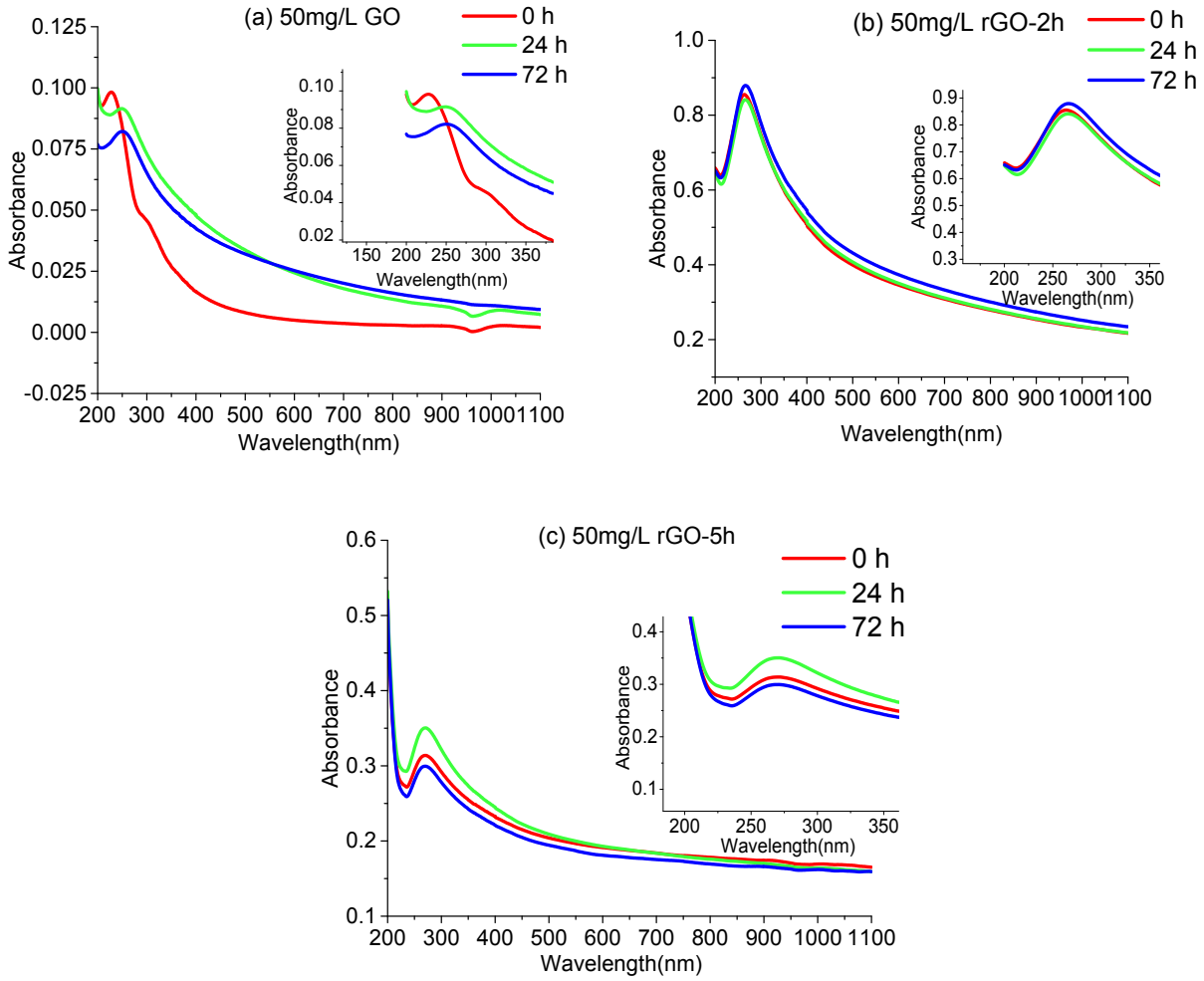

Figure 4. Optical absorbance spectra of irradiated (a) GO, (b) rGO-2h, (c) rGO-5h samples. The shift in the major peak from 230 nm to 270 nm in GO implies the restoration of the graphene lattice, and the disappearance of the peak at 300 nm indicates the removal of oxygen-containing functional groups in GO. No significant changes are observed in the optical absorbance spectra for the rGO materials after irradiation.

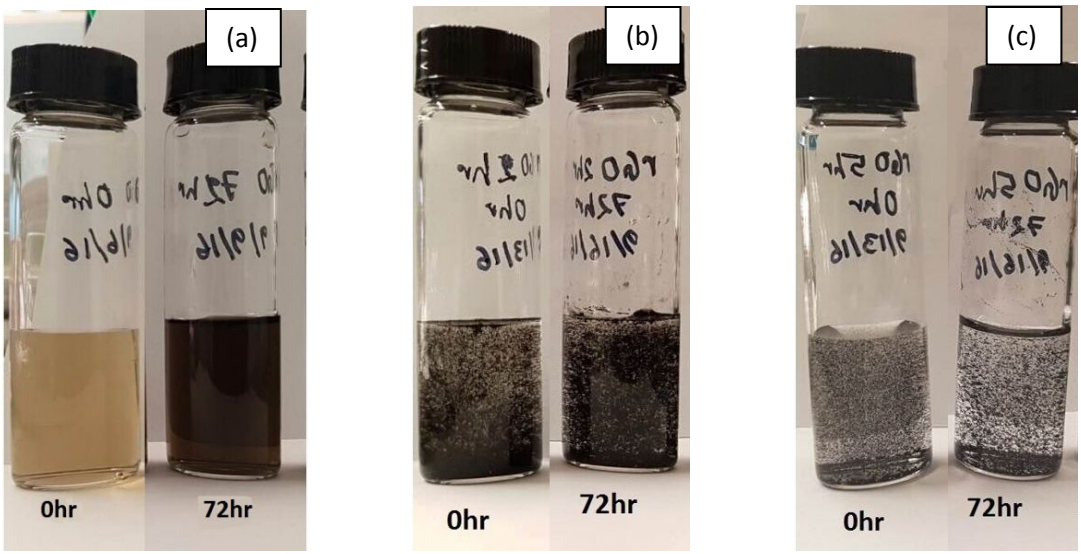

Figure 5. Photographs of (a) GO, (b) rGO-2h, and (c) rGO-5h dispersions before (0 h) and after (72 h) sunlight exposure. The darkened color of the GO dispersion after 72 h of sunlight exposure is indicative of chemical and physical degradation. In contrast, the more hydrophobic rGO materials form aggregates in water, reducing the opportunity for photodegradation.

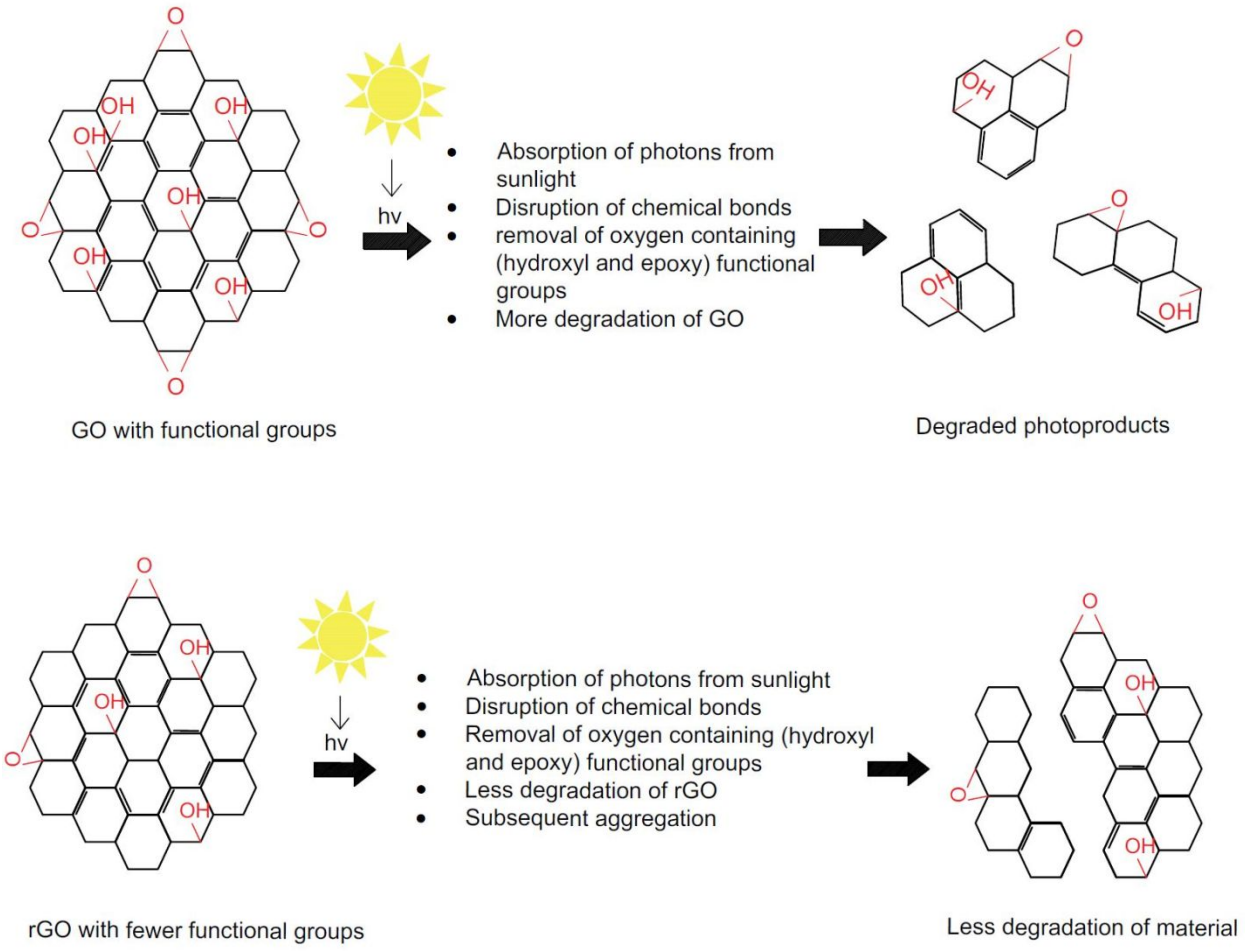

Figure 6. Schematics of the proposed reaction pathway for graphene oxide nanomaterial degradation. Above, GO is shown with oxygen-containing (hydroxyl and epoxy) functional groups. Due to absorption of photons from sunlight, the functional groups are removed, accelerating the physical degradation. Below, rGO with fewer functional groups, undergoes reduced degradation than GO under similar irradiation.

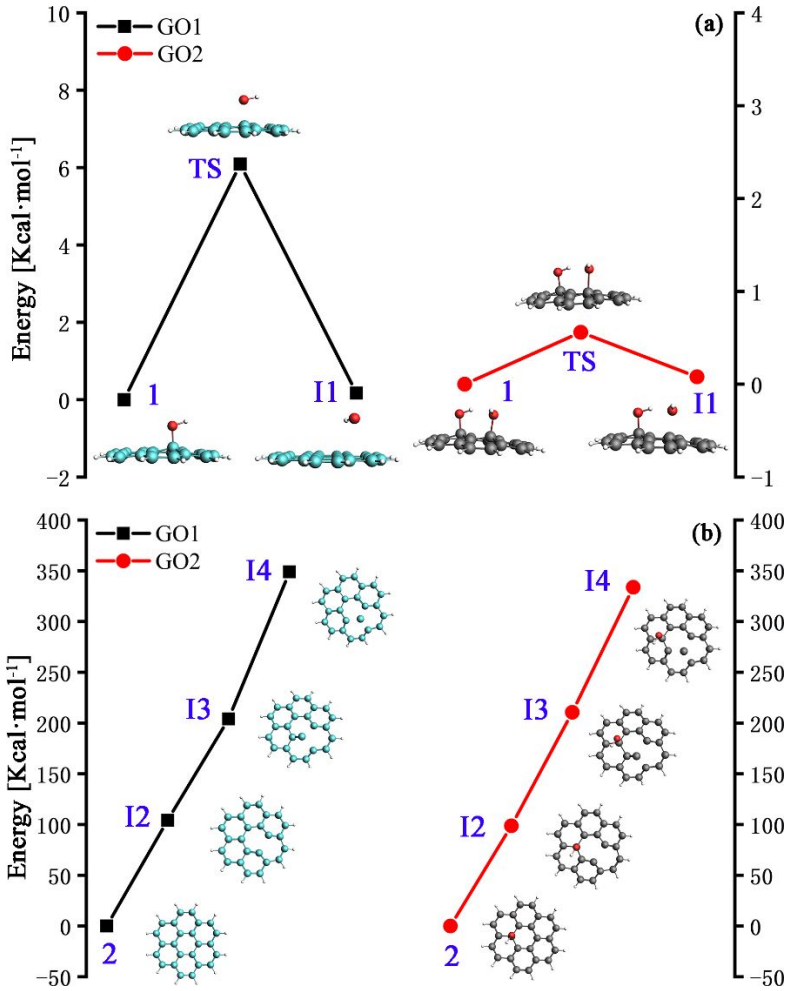

Figure 7. Energetic profiles of the structure degradation for GO (denoted as GO2) and rGO (denoted as GO1) with various oxidization degrees.（a）Potential energy surface plots for the removal of hydroxyl group from GO1 and GO2, respectively. (b) Potential energy curve for the breakage of three C-C bonds in three consecutive steps.Here, O, red; H, white; C on GO1 and GO2 is green and gray, respectively.

TOC Art

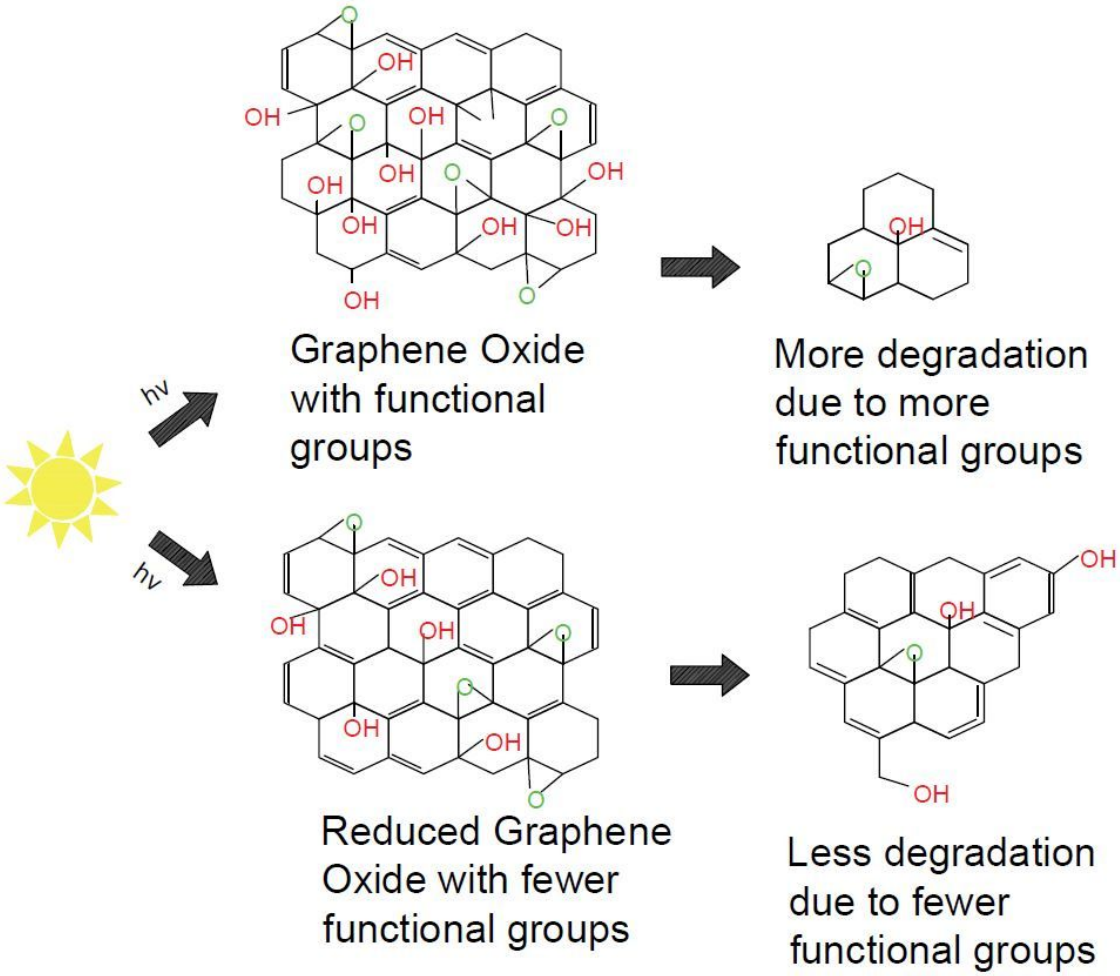
hv
hv
Graphene Oxide with functional groups
More degradation due to more functional groups
Reduced Graphene Oxide with fewer functional groups
Less degradation due to fewer functional groups